Eur Biophys J (2003) 32: 437–449
DOI 10.1007/s00249-003-0316-9

ARTICLE

**Georges Pavlov · Stéphanie Finet · Karine Tatarenko
Evgueniya Korneeva · Christine Ebel**

Conformation of heparin studied with macromolecular hydrodynamic methods and X-ray scattering

Received: 15 December 2002 / Revised: 18 February 2003 / Accepted: 8 April 2003 / Published online: 3 July 2003

Abstract The hydrodynamic characteristics of heparin fractions in a 0.2 M NaCl solution have been determined. Experimental values varied over the following ranges: the sedimentation coefficient (at 20.0 °C), $1.3 < s_0 \times 10^{13} < 3.2$ s; the Gralen coefficient (sedimentation concentration-dependence parameter), $10 < k_s < 70$ cm^3 g^{-1}; the translational diffusion coefficient, $3.9 < D_0 \times 10^7 < 15.4$ cm^2 s^{-1}; the intrinsic viscosity, $7.9 < [\eta] < 40$ cm^3 g^{-1}. Combination of s_0 with D_0 using the Svedberg equation yielded molecular weights in the range $3.9 < M \times 10^{-3} < 37$ g mol^{-1}. The value of the mass per unit length of the heparin molecule, M_L, was determined using the theory of hydrodynamic properties of a weakly bending rod, giving $M_L = 570 \pm 50$ g nm^{-1} mol^{-1}. The equilibrium rigidity, Kuhn segment length ($A = 9 \pm 2$ nm) and hydrodynamic diameter ($d = 0.9 \pm 0.1$ nm) of heparin were evaluated on the basis of the worm-like coil theory without the excluded volume effect, using the combination of hydrodynamic data obtained from fractions of different sizes. Small-angle X-ray scattering for three heparin fractions allowed an estimate for the cross-sectional radius of gyration as 0.43 nm; from the evolution with the macromolecule contour length of the radius of gyration, a value for the Kuhn segment length of 9 ± 1 nm was obtained. A good correlation is thus observed for the conformational parameters of heparin from hydrodynamic and X-ray scattering data. These values describe heparin as a semi-rigid polymer, with an equilibrium rigidity that is essentially determined by a structural component, the electrostatic contribution being negligible in 0.2 M NaCl.

Keywords Heparin · Hydrodynamic characteristics · X-ray scattering

Presented at the conference for Advances in Analytical Ultracentrifugation and Hydrodynamics, 8–11 June 2002, Grenoble, France

G. Pavlov · K. Tatarenko · E. Korneeva · C. Ebel (✉)
Laboratoire de Biophysique Moleculaire,
Institut de Biologie Structurale, UMR 5075 CEA-CNRS-UJF,
41 rue Jules Horowitz, 38027 Grenoble, France
E-mail: christine.ebel@ibs.fr
Tel.: +33-4-38789638
Fax: +33-4-38785494

G. Pavlov
Institute of Physics, St. Petersburg University,
Ulianovskaya str. 1, 198504 St. Petersburg, Russia

S. Finet
European Synchrotron Radiation Facility,
BP 220, 38043 Grenoble, France

E. Korneeva
Institute of Macromolecular Compounds,
Russian Academy of Science,
Bolshoi pr. 31, 199004 St. Petersburg, Russia

Introduction

Heparin is a linear polysaccharide that is heterogeneous in length and composition. It is presented in Fig. 1. It belongs to the glycosaminoglycan family (GAG) isolated from animal tissues. This GAG is a well-known anticoagulant and antithrombotic agent and also affects the growth and biological activities of cells in culture (Casu 1985; Lane et al. 1992; Hileman et al. 1998; Lindahl 2000; Sugahara and Kitagava 2000; Casu and Lindahl 2001). Heparin is also very often used as a model of heparan sulfate (HS). HS contains all of the structural motifs found in heparin, but possesses alternate domains with a high and a low number of charges (Hileman et al. 1998; Mulloy and Forster 2000; Sugahara and Kitagava 2000; Lortat-Jacob et al. 2002). HS is found at the surface or in the extracellular matrix of most animal cells and is involved in various fundamental biological functions such as growth control, the regulation of cell adhesion and morphology, and lipid metabolism, through its interactions with proteins. HS is described as stimulating the response to viral infection (Lortat-Jacob et al. 1996), but also functions as the receptor for a number of pathogens (Spillmann 2001; Liu and Thorp 2002). It can promote or inhibit tumor

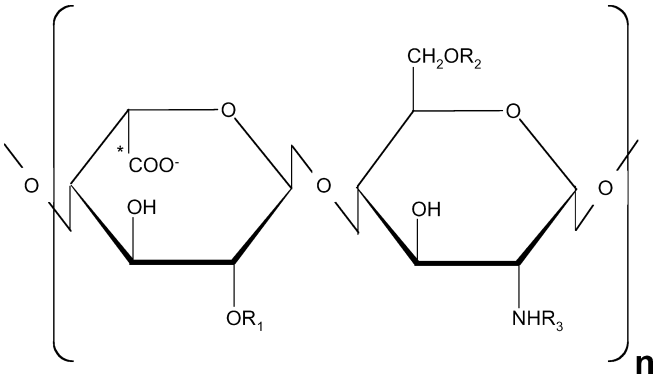

Fig. 1 Structure of repeat units of heparin chains. Heparin chains are based on alternating 1 → 4-linked residues of a uronic acid [generally α-L-iduronic acid (IdoA) represented here, rarely β-D-glucuronic acid (GlcA), which differ from the position of the carboxyl group (*) relative to the plane of the sugar] and D-glucosamine (GlcN). The sugars are heterogeneously substituted: R_1, R_2 = H or SO_3^-; R_3 = H, $COCH_3$ or SO_3^-. The sequence [-4)-α-L-IdoA2(OSO_3^-)-(1 → 4)-α-D-GlcNSO_3^-,6(OSO_3^-)-(1-] usually accounts for more about 80% of heparin

growth and metastasis (Liu at al. 2002). Very often, short fragments of heparin are used to study the molecular structure of proteins for their interactions with HS. Our general aim is to characterize the conformational changes upon protein–heparin or protein–HS interactions. For this purpose, we need fractions of heparin of various lengths and their characterization in terms of conformations in solution, in the absence of proteins. The biophysical characterization (molar mass, polydispersity, intrinsic viscosity) of heparin in solution was essentially performed with small fragments used in clinical applications (Lane and Lindahl 1989; Nieduszynski 1989; Mulloy et al. 1997). In the present work we have studied the relations between the hydrodynamic or scattering characteristics and molecular weights of fractionated heparin in 0.2 M NaCl, using analytical ultracentrifugation, viscosity, density and small-angle X-ray scattering, in order to determine its conformational parameters.

Materials and methods

Heparin sample, elementary analysis, fractionation, dialysis and solvent

Heparin sodium salt from porcine intestinal mucosa was obtained from Sigma (H-3393, lot 98H0713). The elemental analysis was performed by the Service Central d'Analyse, CNRS, at Vernaison, France, after storage in a desiccator under P_2O5 (loss of weight on drying was 0.1%). The heparin sample was fractionated by gel permeation chromatography in 0.2 M NaCl on Sepharose CL6B gel (Pharmacia Biotech) (height, 1 m; diameter, 2.5 cm). Typically, 10 mL at 20 mg mL^{-1} were eluted at 2.5 mL min^{-1} at room temperature and recovered by 5 mL. Four injections were made, the identical fractions gathered together and fractions consisting of 2 or 3 tubes dialysed against H_2O (Spectra-Por 1000 Da) and lyophilized. All subsequent measurements were performed at 20 °C after their solubilization in 0.2 M NaCl (density $\rho_0 = 1.0070$ g $cm^{-3}$and viscosity $\eta_0 = 0.999$ cP).

Sedimentation velocity experiments

Analytical ultracentrifugation was performed on a Beckman XL1 with a rotor speed of 57,000 rpm in a double-sector cell of optical path 12 mm using interference optics. Sedimentation coefficients, s, were evaluated from the displacement of the maxima of the derivatives of the integral distribution (Tanford 1961; Tsvetkov et al. 1970; Cantor and Schimmel 1980). Linear fitting of $s^{-1} = s_0{}^{-1}(1 + k_s c + ...)$ allowed the determination of the coefficients at infinite dilution, s_0, and Gralen coefficients, k_s, where c is the heparin concentration (g cm^{-3}).

Determination of diffusion coefficients and refractive index increments

Translational diffusion was studied by low-speed analytical ultracentrifugation experiments (3000 rpm) with artificial boundary cells of 12 mm path. The diffusion boundary dispersions, σ^2, were calculated using the maximal ordinate, H_{max}, and area, Q, of the derived curves, which were of symmetrical character: $\sigma^2 = (1/2\pi)(Q/H_{max})^2$ (Tanford 1961; Tsvetkov et al. 1970). The translational diffusion coefficient, D, was determined from $\sigma^2 = \sigma_0{}^2 + 2Dt$, where $\sigma_0{}^2$ is the initial dispersion characterizing the quality of diffusion boundary formation. The diffusion coefficient at infinite dilution, D_0, was estimated from measurements at different heparin concentrations (see the Results section). Q was also used to derive the total number of fringes, J, corresponding to the heparin concentration in solution, from which was calculated its refractive index increment: $(\Delta n/\Delta c) = J\lambda/Kcl$, where λ is the wavelength (675 nm), K the magnifying coefficient and l the optical path. From measurements of NaCl solutions in the range $(1.2–10.5)\times10^{-2}$ g cm^{-3} (checked by density), for which the relationships between concentration and Δn values are tabulated (Weast 1975), we used $\lambda/Kl = 5.70\times10^{-5}$, which is the mean value between that determined experimentally in our centrifuge ($\lambda/Kl = 5.77\times10^{-5}$) and that expected ($5.625\times10^{-5}$for $K = 1$ and $l = 12$ mm).

Intrinsic viscosity measurements

Viscosity measurements were made at 20.0 °C using an AMV 200 rolling ball viscometer with a manually filled capillary of internal diameter 0.8 mm, recommended for the range 0.5–5 cP (Anton Paar, Graz, Austria). The viscosities of the solution, η, and of the solvent, η_0, were obtained from the rolling times of the steel ball for the solution, t, and solvent, τ_0, measured at four inclination angles (from 40° to 70°) of the capillary. We used the average ratio $\eta/\eta_0 = t/\tau_0$ to determine the specific viscosities: $\eta_{sp} = (\eta - \eta_0)/\eta_0$. The intrinsic viscosities, $[\eta]$, of the heparin fractions were determined from the plots $\eta_{sp}/c = [\eta] + k'[\eta]^2 c + ...$, where k' is the Huggins' parameter.

Density measurements

The density increment $\Delta\rho/\Delta c$, where $\Delta\rho$ is the difference between the densities of the heparin solution and solvent, was measured using unfractionated heparin, with a DMA 5000 density meter (Anton Paar, Graz, Austria) according to the procedure of Kratky et al. (1973).

Small-angle X-ray scattering

The SAXS experiments were carried out on the fractions 4, 8, and 11, each at two or three concentrations of typically 6, 12 and 20 mg mL^{-1}, using the high brilliance beamline ID2 at the European Radiation Synchrotron Facility in Grenoble, France (Narayanan et al. 2001). The experiments were performed at room

temperature using the ID2 flow-through cell (2 mm diameter and 10 μm thickness quartz capillary, from GLAS) operated under vacuum that could be filled and rinsed in situ. The sample volume was 50 μL. Data were collected using a two-dimensional detector (X-ray image intensifier coupled to an ESRF-developed FReLoN CCD camera, 1024×1024 pixels). The sample-to-detector distance was 2.5 m, yielding a Q increment per channel of 0.00419 nm^{-1}, with $Q = 2\pi s = 4\pi \sin\theta/\lambda$, where s is scattering vector, λ the wavelength of the X-ray and 2θ the scattering angle. With $\lambda = 0.0995$ nm, the useful Q range was $0.15 < Q < 2.6$ nm^{-1}. The two-dimensional data reduction consists of (1) normalization to the detector response, the exposure time and the sample transmission, (2) absolute intensity calibration, (3) masking of the beamstop and the border regions, (4) azimuthal integration and averaging, and (5) background subtraction and sample concentration normalization. The exposure time was 0.1 and 0.5 s and 10 curves were averaged, giving the same results; no radiation damage was observed.

Theoretical background

Parameters characterizing the conformation of linear polymers

A linear polymer fraction is characterized by its molecular weight, M, contour length, L, mean-square end-to-end distance, $<h^2>$, or mean-square radius of gyration, $<R_g{}^2>$ (Tanford 1961; Tsvetkov et al. 1970). In the Gaussian coil limit, $<h^2>$ and $<R_g{}^2>$ are related in a simple way: $<h^2> = 6<R_g{}^2>$. The hydrodynamic diameter, d, the persistence length, a, or the Kuhn segment length, $A = 2a$, and the value of the mass per unit length, $M_L = M/L$, are parameters that are common for a series of homologous linear polymers.

Relationships between the experimental hydrodynamic values and the macromolecular characteristics

The different experimental measurements can be expressed as intrinsic values, $[\eta]$, $[D]$, $[s]$, k_s, which are independent of the solvent properties. Each of them is related to common macromolecular characteristics, which are, in the case of linear polymers, M and $<h^2>$ (Svedberg and Pedersen 1940; Tanford 1961; Tsvetkov et al. 1970; Yamakawa 1971; Cantor and Schimmel 1980):

$$[\eta] = \Phi <h^2>^{3/2}/M \tag{1}$$

$$[D] \equiv D_0\eta_0/T = k/(P<h^2>^{1/2}) \tag{2}$$

$$[s] \equiv s_0\eta_0/(\Delta\rho/\Delta c) = M/(P<h^2>^{1/2}N_A) \tag{3}$$

$$k_s = B<h^2>^{3/2}/M \tag{4}$$

where T is the absolute temperature, k is Boltzmann's constant and N_A is Avogadro's number. For polyelectrolytes in the presence of complex solvents, since solvent redistribution close to the macromolecules is possible, then $(\Delta\rho/\Delta c) = (1 - \rho^\circ\phi')$ is used to obtain an operational apparent specific volume (ϕ') without thermodynamic significance, ρ° being the solvent density. Φ and P are the Flory hydrodynamic parameters; B is also a hydrodynamic dimensionless parameter. The values of Φ and P are functions of the relative contour length (L/A) and relative diameter (d/A), tabulated in the case of the worm-like cylinder theory (Yamakawa and Fujii 1973, 1974). They are related to the rigidity and length of the polymer (and also to the thermodynamic quality of the solvent related to long-chain interactions; in the present study, heparin chains are rather short with $L/A \leq 10$ and this term will not be considered). In the case of linear polymers, the sensitivity to the changes in the molecular weight decreases in the order: Eq. (1)≈Eq. (4) > Eq. (2) > Eq. (3). Combining $[D]$, $[s]$ and $[\eta]$ allows us to calculate the hydrodynamic invariant, A_0 (Mandelkern and Flory 1952; Tsvetkov and Klenin 1953):

$$A_0 \equiv k(\Phi_0/100)^{1/3}P_0^{-1} = \{R[D]^2[s][\eta]\}^{1/3} \tag{5}$$

where $R = kN_A$ and $[\eta]$ is in dL g^{-1}. Combining $[D]$, $[s]$ and k_s allows us to calculate the sedimentation parameter, β_s (Pavlov and Frenkel 1995; Pavlov 1997):

$$\beta_s \equiv B^{1/3}/P = N_A\{R^{-2}[D]^2[s]k_s\}^{1/3} \tag{6}$$

The ratios $\Phi^{1/3}/P$ and $B^{1/3}/P$, and thus A_0 and β_s, even if not theoretically strictly constant, are experimentally found to be invariant (i.e. within the incertitude of the measurements) in the case of polymers of homologous structure but different lengths. The limiting theoretical values of Φ and P for a Gaussian coil ($M \to \infty$), obtained after a preliminary averaging of the hydrodynamic Oseen's tensor, are $\Phi_0 = 2.87\times10^{23}$and $P_0 = 5.11$ (Yamakawa 1971; Tsvetkov 1989). The theoretical values of the Flory hydrodynamic parameters P_0 and Φ_0 depend on the models and mathematical approximations. They are affected by the preaveraging of the Oseen hydrodynamic tensor, as studied by the Monte-Carlo simulation method (Zimm 1980; Garcia de la Torre et al. 1984) and by renormalization group calculations (Oono and Kohmoto 1983), leading to limiting values of 6.0 or 6.2 for P_0 and 2.5 or 2.36×10^{23} for Φ_0, respectively.

Scaling relations between the hydrodynamic values and molecular weight

For homologous polymers, all the hydrodynamic values and molecular weights may be related through scaling relations of the Kuhn–Mark–Houwink–Sakurada type:

$$P_i = K_{ij}P_{j\neq i}^{bij} \tag{7}$$

where P_i, $P_{j\neq i}$ are $[\eta]$, s_0, D_0, k_s and P_j may also be M. In the case of linear polymers, the scaling indices b_{ij} are intercorrelated (Tsvetkov et al. 1970; Pavlov and Frenkel 1995).

Relationship between hydrodynamic values and conformational parameters A and d in the model of a worm-like chain

In the limit of low molecular weight chains ($L/A < 2.3; L >> d$), a model of a weakly bending rod or a cylinder can be used that provides M_L and d through a linear regression (Broersma 1969; Yamakawa and Fujii 1973):

$$[s] = (M_L/3\pi N_A)[\ln M - \ln(M_L d) + 0.3863] \tag{8}$$

For larger molecular weight chains in the limit $L/A > 2.28$, and without intramolecular volume interactions, A and d can be obtained by linear regressions relating $[s]$ and M [Hearst and Stockmayer (1962) and Yamakawa and Fujii (1973) theories (Tsvetkov 1989)]:

$$[s]N_AP_0 = (M_L/A)^{1/2}M^{1/2} + (P_0M_L/3\pi)[\ln(A/d) - \varphi(0)] \tag{9}$$

where $\varphi(0) = 1.431$ or 1.056 considering a worm-like necklace (Hearst and Stockmayer 1962) or worm-like cylinder (Yamakawa and Fujii 1973), respectively. A similar equation relating $[\eta]$ and M [Bushin's plot (Bushin et al. 1981; Tsvetkov 1989)] is based on the reasonable assumption that the same macromolecular dimensions are measured in the translational and rotational frictions, i.e. $<h^2>_f = <h^2>_\eta = <h^2>$ in Eqs. (1) and (2) or (3). Thus:

$$\begin{aligned}(M^2\Phi_0/[\eta])^{1/3} &= [s]P_0N_A \\ &= (M_L/A)^{1/2}M^{1/2} + (P_0M_L/3\pi)[\ln(A/d) - \varphi(0)]\end{aligned} \tag{10}$$

Pavlov and Frenkel (1995) used also Eqs. (3) and (4) to relate $[s]$ and k_s, through the invariant sedimentation parameter β_s, in a form similar to Eq. (9):

$$[s]P_0N_A = (N_A/\beta_s)^{3/4}(M_L/A)^{1/2}[s]^{3/4}k_s^{1/4}+(P_0M_L/3\pi)[\ln(A/d) - \varphi(0)] \quad (11)$$

It can be noted that Eqs. (9)–(11) use the Φ_0 and P_0 values of a Gaussian coil, but without precluding that the data correspond to Gaussian chains. Also, the comparison of the values of equilibrium rigidity of different polymers requires that they are estimated using the same sets of the hydrodynamic parameters Φ_0 and P_0.

Dimensional characteristics obtained from the small-angle X-ray scattering of polymer molecules in solution

The normalized intensities $I(Q)$ were used, in the limit $QR_g \leq 1.3$, in the Guinier approximation (Guinier and Fournet 1955):

$$I(Q) = I_0\exp(-Q^2<R^2_{gapp}>/3) \quad (12)$$

From linear fitting, I_0 and $R_{g\ app}$, the intensity extrapolated at zero angle and the apparent radius of gyration of the molecule, are obtained. The radius of gyration, R_g (strictly $<R_g{}^2>^{1/2}$), and forward intensity at infinite dilution, I_{00}, were obtained from the linear extrapolation of $R^2g_{\ app}$ and $1/I_0$at zero heparin concentration. The latter plot also provides a value for the second virial coefficient A_2 (in mol mL g^{-2}) since $1/I_0 = 1/I_{00} + 2A_2Mc/I_{00}$ can be derived from the virial expansion of the osmotic pressure, neglecting virial coefficients of order higher than two (Costenaro et al. 2001). The Guinier approximation can be written as:

$$I(Q)Q = (IQ)_0\exp(-Q^2R_c^2/2) \quad (13)$$

for rod-like molecules, in the limit of $QR_c >> 1$, where $(IQ)_0$ refers to the extrapolated product $I(Q)Q$ at zero angle, and R_c to the cross-section radius of gyration of the polymer chain. We used it in the range $1.2 \leq Q \leq 2.3$. The ratio $I_{00}/(IQ)_0$ gives the contour length (L) of the macromolecule (Glatter and Kratky 1982; Lindner and Zemb 1991):

$$L = \pi I_{00}/(IQ)_0 \quad (14)$$

For a homologous series of linear polymers, the mean-square radius of gyration, R_g, is related across the whole range of molecular weights to the ratio of the contour length, L, and the persistence length, a, by the following relationship (Benoit and Doty 1953; Landau and Lifschitz, 1963):

$$R_g^2 = a^2\{(L/a)/3 - 1 - [2/(L/a)][1 - \{1 - \exp[-(L/a)]\}/(L/a)]\} \quad (15)$$

Electrostatic contribution to the polymer rigidity

The concept of stiffness additivity is accepted (Mandel 1993; Barrat and Jonny 1996) and the total chain Kuhn segment length can be written as the sum of the structural, A_{str}, and electrostatic, A_{el}, components, which depend on the structure of the repeat unit of the polymer and the ionic strength of solution, and on the linear charge density of the polymer, respectively:

$$A_{tot} = A_{str} + A_{el} \quad (16)$$

The Debye–Hückel screening length, $\kappa^{-1} = (8\pi\lambda_B\mu)^{-1/2}$, characterizes the screening action of the solvent. It is related to its Bjerrum length, $\lambda_B = (e^2/4\pi\epsilon_0\epsilon kT)$, and its ionic strength, μ, where e is the elementary charge, ϵ_0 is the absolute dielectric constant, ϵ is the dielectric constant of the medium, and $\mu = C\times10^{-3}\times N_A$ cm^{-3} in the case of NaCl solutions of molar concentration C. The linear polymer is characterized by a dimensionless charge parameter, Q_{el}, which is the ratio of Bjerrum length to the average contour length per unit charge, L/Z:

$$Q_{el} = \lambda_B/(L/Z) = \lambda_BZ/L \quad (17)$$

The general expression for A_{el} derived by Odijk (1977) also uses a correction factor, f^2, to take into account the reduction of the effective charge density due to counterion condensation ($f^2 < 1$), and a function, $F(\kappa L)$, which depends on the reduced contour length, κL [for $\kappa L >> 1$, $F(\kappa L) = 1$]:

$$A_{el} = (Q_{el}^2/2\lambda_B\kappa^2)f^2F(\kappa L) \quad (18)$$

which reduces, when $Q_{el} > 1$, to:

$$A_{el} = \kappa^{-2}/2\lambda_B \quad (19)$$

Results

Chemical analysis

The ratio between the sulfur and nitrogen contents, $S = 8.8 \pm 0.3\%$ and $N = 1.80 \pm 0.07\%$, was used to calculate the mean number of sulfate groups as 2.14 per disaccharide, and the mean molecular weight for the disaccharide of 580 g mol^{-1}.

Fractionation of heparin

Preparative gel permeation chromatography allowed us to obtain 510 mg of heparin from 800 mg of loaded material, in 14 fractions of different heparin size, as can be seen from polyacrylamide gel electrophoresis (see Fig. 2). Their weights were from a minimum of 1.5 mg (fraction 1) to more than 70 mg.

Refractive index increments of heparin

In Fig. 3 the total number of fringes as a function of heparin concentration is superimposed for all the heparin fractions, including the unfractionated sample. From the linear plot of all the points we derive $(\Delta n/\Delta c) = 0.132 \pm 0.001$ cm^3 $g^{-1}$for heparin, in agreement with the published values of 0.129–0.134 (Knobloch and Shakllee 1997), 0.128 (Loucas et al. 1971) and 0.126–0.137 (Miklautz et al. 1986; Theisen et al. 2000). Also, the fact that all points nicely superimpose is an indication that all the heparin fractions are chemically homologous.

Results of analytical ultracentrifugation and viscosity measurements

All experiments were performed in the "dilute" regime, with a heparin concentration below 11 mg mL^{-1} (analytical ultracentrifugation) or 25 mg mL^{-1}(viscosity). The upper limits of the dilute regime can be defined as $C^* = 3\ M/N_A4\pi Rg^3 \approx 1.7/[\eta]$ (Gotlib et al.1986), or in a more restrictive way as $C^* \approx [\eta]^{-1}$. The latter corresponds, for the examples of fractions 1 and 12, to 25 and 110 mg mL^{-1}, respectively. The concentration

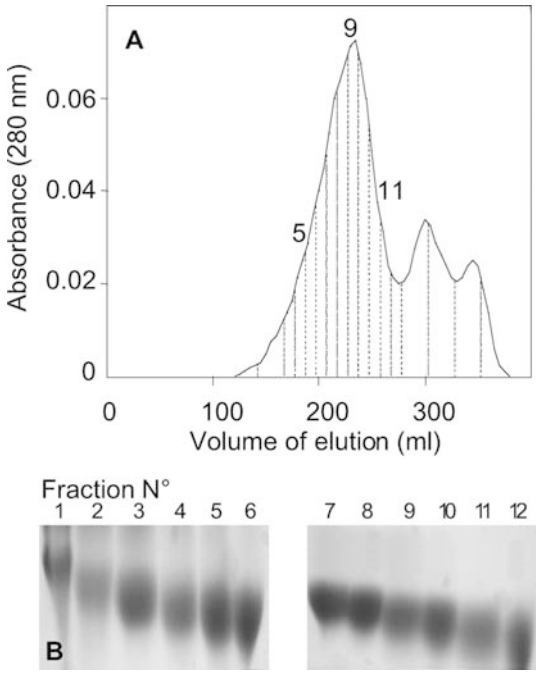

Fig. 2 Fractionation of heparin. 10 mL of heparin at 200 mg mL^{-1} were loaded on a column of Sepharose CL6B (25×1000 mm) at room temperature at the rate of 2.5 mL min^{-1} and tubes of 5 mL were recovered. **A** The absorbance profile was measured at 280 nm. Heparin absorbance maximum is at 210 nm; $A_{280}/A_{210} = 0.14$. Two to five tubes were pooled and 17 fractions obtained (separated on the figure by *vertical bars*). For clarity, the position of only fractions 5, 9 and 11 is indicated. **B** 15% polyacrylamide gel electrophoreses in Tris-glycine (without SDS) of the fractions 1–12. Bromophenol blue was used to follow the migration, and heparin revealed on the gels with aqueous 0.08% Azure A. The fractions 15–17 corresponding to the two minor peaks of **A** are contaminants since they did not contain heparin (data not shown)

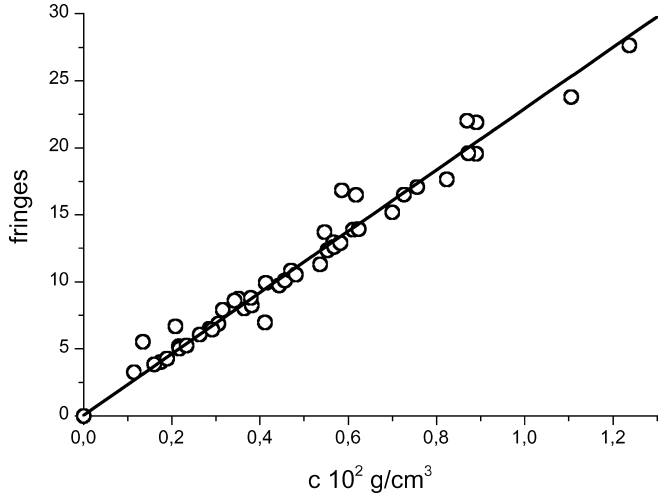

Fig. 3 The total number of fringes vs. concentration of heparin in 0.2 M NaCl solution. The refractive index increment was calculated according to the following relation: $\Delta n/\Delta c = 5.7\times10^{-5}(J/c)$, where J is the total number of fringes. For a path-length of 12 mm in the ultracentrifuge and $\Delta n/\Delta c = 0.1$ cm^3 g^{-1}, a concentration of 1 mg mL^{-1}corresponds to 1.75 fringe

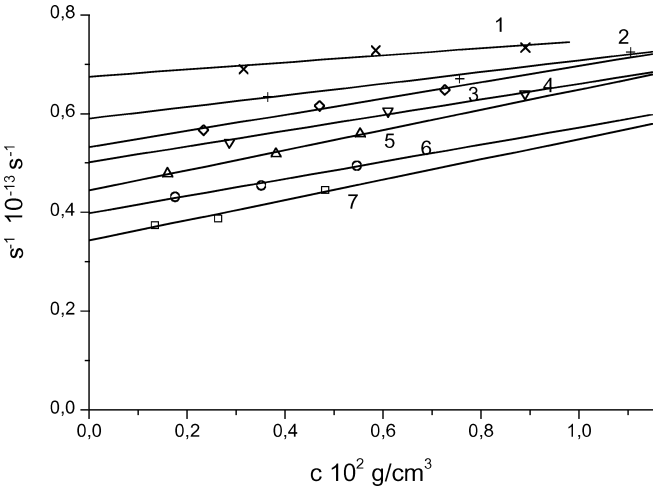

Fig. 4 Concentration dependencies of the (reciprocal) sedimentation coefficient s^{-1} for heparin fractions in 0.2 M NaCl. The numbers *1* to *7* correspond to fractions 13, 12, 11, 10, 8, 4 and 2, respectively

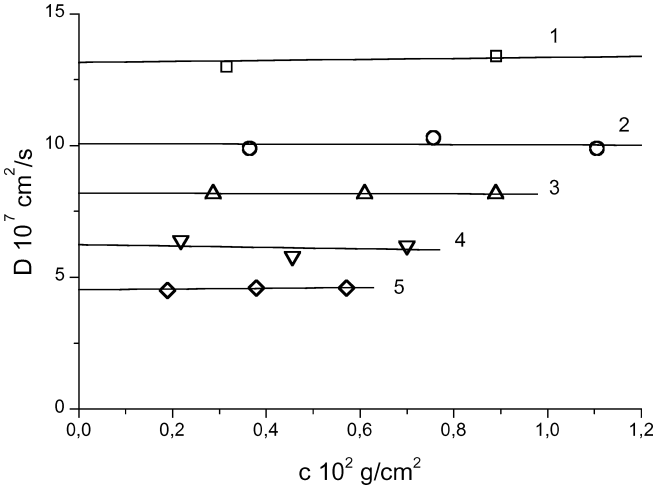

Fig. 5 Concentration dependencies of the diffusion coefficient D for heparin fractions in 0.2 M NaCl. The numbers *1* to *5* correspond to fractions 13, 12, 10, 5 and II, respectively

dependencies of the reciprocal sedimentation coefficients always satisfied the linear approximation, as can be seen in Fig. 4. The values of the measured diffusion coefficients, D, did not vary with the heparin concentrations (see Fig. 5). The plots of η_{sp}/c as a function of c allowed us to determine the intrinsic viscosities, $[\eta]$, of the heparin fractions (Fig. 6). Table 1 presents the values of s_0, k_s, D_0 (which is the mean experimental value for the different concentrations) and $[\eta]$.

Determination of the buoyancy factor and molar masses of the fractions

Figure 7 shows the superposition of the density measurements for heparin prepared in three different ways.

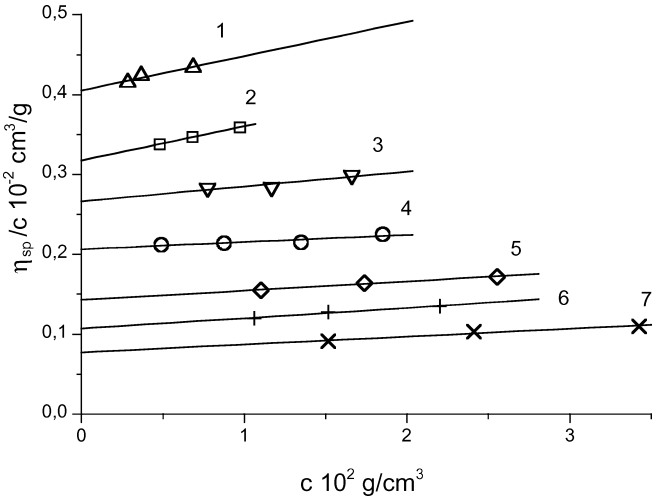

Fig. 6 Plots of η_{sp}/c vs.c for heparin solutions in 0.2 M NaCl at 20 °C. The numbers *1* to *7* correspond to fractions 1, 2, 4, 8, 10, 11 and 12, respectively

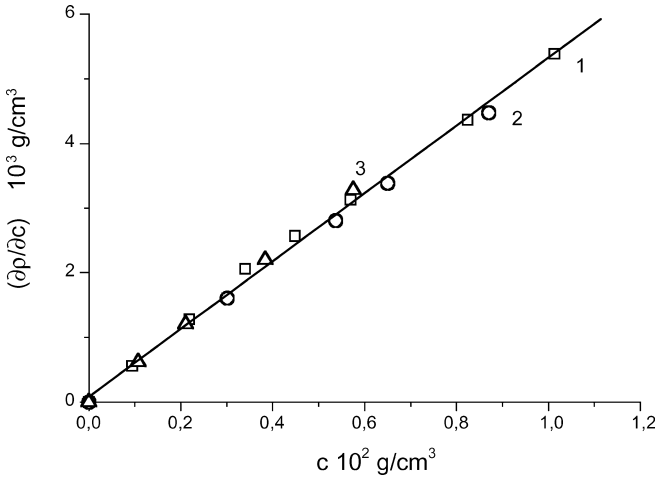

Fig. 7 Density increment $\Delta\rho/\Delta c$ of heparin in 0.2 M NaCl and water at 20 °C. $\Delta\rho = \rho - \rho_0$, where ρ and ρ_0 are the solution and solvent densities, respectively, for: *1* (*squares*) solutions before dialysis in 0.2 M NaCl;*2* (*circles*) solutions after dialysis in 0.2 M NaCl; *3* (*triangles*) solutions in pure water

No significant differences are found for heparin diluted in or dialysed against 0.2 M NaCl and heparin diluted in H_2O. The derived buoyancy factor ($\Delta\rho/\Delta c$) is 0.530 ± 0.008, corresponding to an apparent partial specific volume of 0.467 cm^3 g^{-1}, which compares well with literature values of 0.50 in phosphate buffer and 0.47 in NaCl buffer (Barlow et al. 1961; Lasker and Stivala 1966). Combining, for each fraction, s_0, D_0 and $\Delta\rho/\Delta c$ in the Svedberg equation:

$$M_{sD} = [RT/(\Delta\rho/\Delta c)]s_0/D_0 \qquad (20)$$

allowed us to determine the mean molar mass, M_{sD}, of the macromolecule. The values are reported in Table 1.

The polydispersity, M_w/M_n, of non-fractionated heparin and fractions 8, 10, 11 and 12 was determined by analytical gel permeation chromatography (details will be given elsewhere) to be 1.28, 1.07, 1.09, 1.10 and 1.11, respectively. These last values correspond in polymer science to samples of very low heterogeneity. It is justifiable to consider fractionated heparin as essentially homogeneous in molecular weight.

SAXS data

As illustrated in Fig. 8 for fraction 8, the X-ray scattering profiles, for the three studied fractions, were strongly dependent on heparin concentration (panel A). The apparent radius of gyration, $R_{g\ app}$, and forward intensites, I_0, were obtained from the Guinier plots at small Qrange [ln$I(Q)$ as a function of Q^2] for each con-

Table 1 Sedimentation coefficient at zero concentration, s_0, Gralen coefficient, k_s, intrinsic viscosity, [η], diffusion coefficient, D_0, molecular weight, M_{sD}, hydrodynamic invariant, A_0, and sedimentation parameter, β_s, of heparin fractions in 0.2 M NaCl at 20 °C

Fraction[a]	$s_0\times10^{13}$(s) (±3%)	k_s (cm^3 g^{-1})	[η] (cm^3 g^{-1}) (±6%)	$D_0\times10^7$ (cm^2 s^{-1}) (±4%)	$M_{sD}\times10^{-3}$ (g mol^{-1}) (±9%)	$A_0\times10^{10}$	$\beta_s\times10^{-7}$
1	3.18	57	40.3	3.95	37.0	3.32	1.25
I	2.92	66	37	3.9	34.4	3.08	1.25
2	2.90	62	32	4.4	30.3	3.21	1.35
II	2.63	70	36	4.55	26.6	3.26	1.37
4	2.51	43	27	5.9	19.6	3.50	1.38
5	2.40	39	23	6.2	17.8	3.38	1.36
III	2.15	24	23	6.2	15.6	3.23	1.35
IV	2.20	26	18.0	7.2	14.1	3.35	1.27
8	2.25	46	20.6	7.55	13.7	3.63	1.59
10	1.99	32	14.5	8.2	11.2	3.29	1.44
11	1.88	31	10.4	9.2	9.4	3.11	1.50
V	1.70	13	12.0	9.0	8.5	3.11	1.08
12	1.69	20	8.5	10.1	7.7	2.99	1.33
13	1.48	10	7.9	13.3	5.1	3.36	1.22
14	1.3	8	–	15.4	3.9	–	1.19
–[b]	2.30	42	21	7.0	14.8	3.47	1.48

[a]Arabic and roman numerals account for two different fractionations
[b]Corresponds to the unfractionated sample

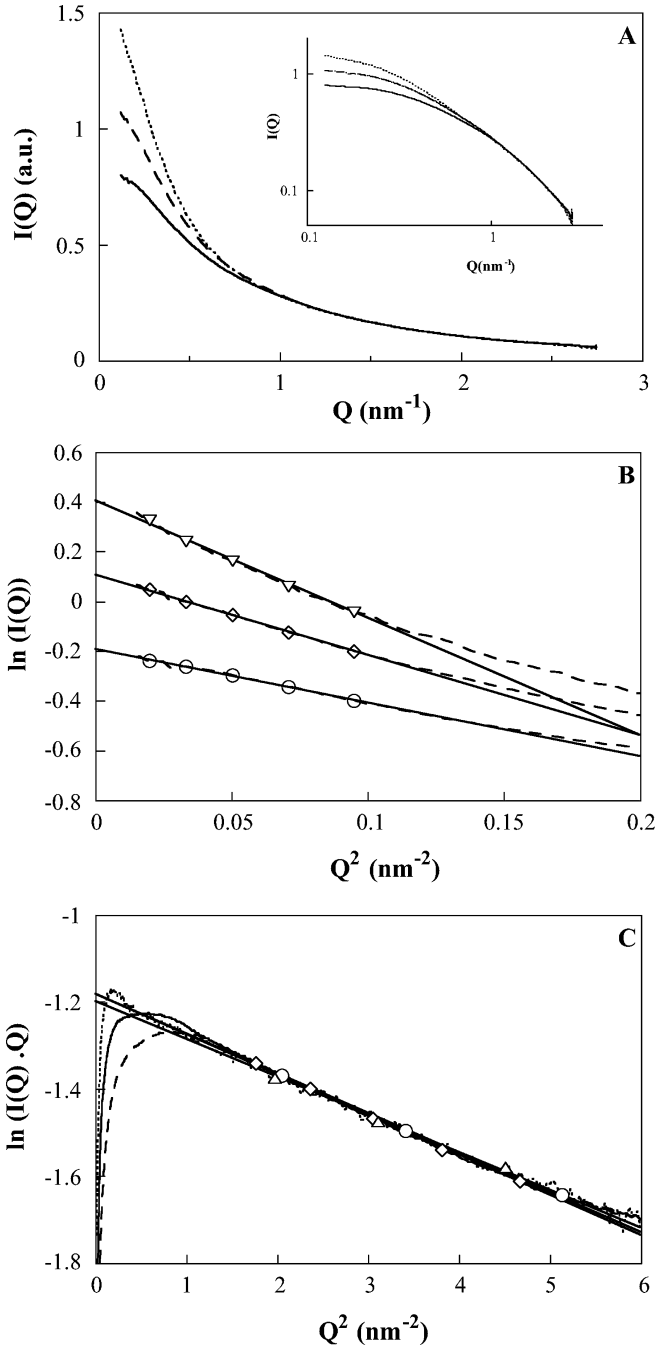

Fig. 8 SAXS of fractionated heparin in 0.2 M NaCl at room temperature. Fraction 8 at 24.8 mg mL^{-1} (*solid line*), 15.0 mg mL^{-1} (*dashed line*) and 7.5 mg mL^{-1} (*dotted line*) are presented. The intensity $I(Q)$ was normalized by heparin concentration. **A** Scattering curves. **B** Guinier plots at low angle, from which $R_{g\ app}$ and I_0 were obtained. **C** Guinier plots at large angle, from which R_c and $(IQ)_0$ were obtained

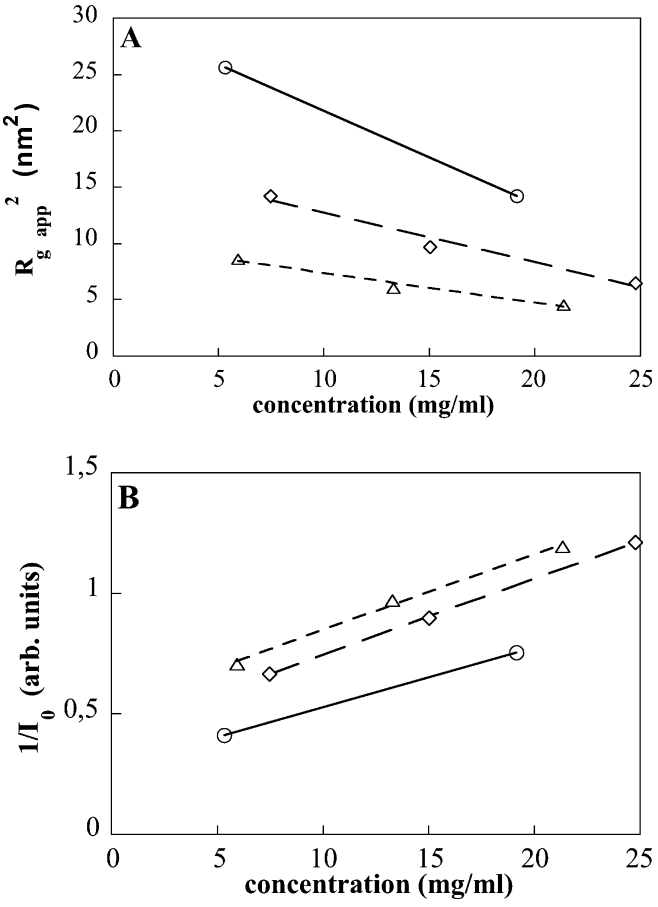

Fig. 9 Linear extrapolation of $R_{g\ app}{}^2$ and $1/I_0$ at infinite dilution. The radius of gyration R_g (**A**) and the forward X-ray intensity I_{00} at infinite dilution and second virial coefficients (**B**) were obtained from the linear fits for the fractions 4 (*circles*), 8 (*diamonds*) and 11 (*triangles*)

centration (panel B). Panel C shows ln $I(Q)Q$ plotted as a function of Q^2 and the very good superimposition of the three curves for the large Q range: the derived cross-section radius of gyration is 0.43 nm and $(IQ)_0$ has a constant value. For fractions 4 and 11, the superimposition (expected to be independent of the fraction size and concentration for a homologous series of linear polymers) was less perfect (probably related to systematic errors). However, the derived mean R_c value was identical: 0.43 ± 0.02 nm after combining all the measurements. Figure 9 shows the concentration dependencies of the square of the apparent radius of gyration, $R_{g\ app}$, and inverse of the forward intensities, $1/I_0$, for the three fractions. Their linear extrapolations at infinite dilution provided the values of R_g, I_{00} and A_2, respectively, for each fraction. We obtain slightly different values from the linear interpolation of I_{00} from I_0 and $1/I_0$. The derived values for $2A_2M$ of 88, 73 and 59 mL g^{-1} for fractions 4, 8 and 11, respectively, are in the same range of magnitude but twice as much as the corresponding k_s values (Table 1). These values were expected to be similar (Solovyova et al. 2001). One reason for the discrepancy could be a systematic overestimation of the stock solutions used in the SAXS experiments. This would not affect the values of the derived dimensional parameters R_g, R_c and L, which are independent of c or derived from extrapolation to infinite dilution values, nor the δ parameter introduced in

Table 2 Radii of gyration (R_g) and contour lengths (L) of heparin fractions from SAXS measurements in 0.2 M NaCl

Fraction	R_g (nm) (± 0.2 nm)	L (nm)[a]
4	5.5	26–33
8	4.2	16–22
11	3.2	15–17

[a]The error in L was estimated from the extrapolations of the X-ray forward intensity or inverse value at infinite dilution

the Discussion (below). The values of I_{00} were combined with the mean $(IQ)_0$ value obtained at different concentrations for each fraction for estimation of the contour length (L). The values of R_g and L for each of the tested fractions are given in Table 2.

Discussion

Heparin fractions as a homologous series

The interpretation of the measurements in term of worm-like chain parameters (persistence length or Kuhn segment length, diameter) requires that all the fractions constitute a homologous series in which the length is the only variable parameter. The constancy of the $\Delta n/\Delta c$ values is in agreement with a constant chemical composition. The hydrodynamic invariants A_0 and β_s were calculated for all fractions, and found to be constant within the experimental uncertainty (see Table 1). This is an indication that all the fractions are structurally homologous. The mean value for A_0 is $3.29 \pm 0.13\times10^{-17}$ J K^{-1} mol$^{1/3}$and for β_s is $1.34 \pm 0.10\times10^{7}$ mol$^{1/3}$. These average values are characteristic for linear polymers (Tsvetkov et al. 1984; Pavlov and Frenkel 1995). Figure 10 shows the dependence of $[\eta]$, s_0 or D_0 on M_{sD} in double logarithmic representation. The values of the linear regression parameter (>0.97) for these plots indicate that the scaling relationships, which are valid for linear homologous polymers, can be defined. The scaling indicesb_{ij} are given in Table 3. The rather good correlation between the different scaling indices is again a characteristic feature of a homologous series of linear polymers. The $[\eta]$–M (Laurent 1961; Lasker and Stivala 1966; Nieduszynski 1989; Knobloch and Shaklee 1997) and s_0–M (Lasker and Stivala 1966; Liberti and Stivala 1967; Nieduszynski 1989) relations have already been investigated for heparin fractions, with similar results for the same solvent ionic strength.

Table 3 Scaling relations between the hydrodynamic values and molecular weight for heparin fractions in 0.2 M NaCl[a]

P_i–P_j[a]	$b_{ij} \pm \Delta b_{ij}$	K_{ij}	r
$[\eta]$–M	0.90 ± 0.06	3.44×10^{-3}	0.975
D_0–M	$-(0.62 \pm 0.01)$	2.57×10^{-4}	−0.996
s_0–M	0.38 ± 0.01	5.64×10^{-15}	0.992
k_s–s_0	2.49 ± 0.24	4.58	0.940
s_0–D_0	$-(0.61 \pm 0.03)$	7.04	−0.978
D_0–$[\eta]$	$-(0.66 \pm 0.05)$	47.2	−0.971
s_0–$[\eta]$	0.40 ± 0.03	0.679	0.967

[a]The properties P_i and P_j of all the fractions are related by: $\log P_i = \log K_{ij} + b_{ij} \log Pj$; r is the linear correlation coefficient. Taking into account experimental errors, it can be seen that the scaling indices b_{ij} are related to each other in the characteristic ways of an homologous series of linear polymers: $b_{s_0-D_0} = b_{s_0-M}/b_{D_0-M}$; $b_{D_0-[\eta]} = b_{D_0-M}/b_{[\eta]-M}$; $b_{s_0-[\eta]} = b_{s_0-M}/b_{[\eta]-M}$; $b_{k_s-s_0} = (2-3b_{s_0-M})/b_{s_0-M}$; $|b_{D_0-M}| = 1/3(1+b_{[\eta]-M})$; $|b_{D_0-M}| + b_{s_0-M} = 1$.

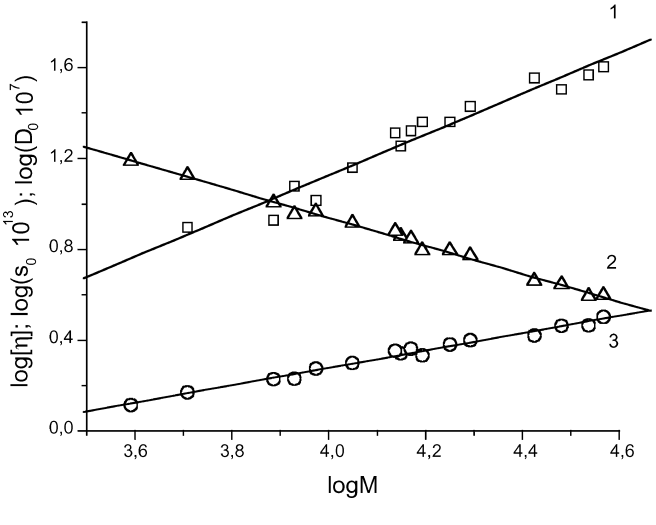

Fig. 10 Scaling plots for heparin molecules in 0.2 M NaCl. The double logarithmic plots of intrinsic viscosity $[\eta]$ (*curve 1*), diffusion coefficient D_0 (*curve 2*) and sedimentation coefficients_0 (*curve 3*) vs. molecular weight $M \equiv M_{sD}$ are plotted. The values of the slopes give the scaling indices reported in Table 3

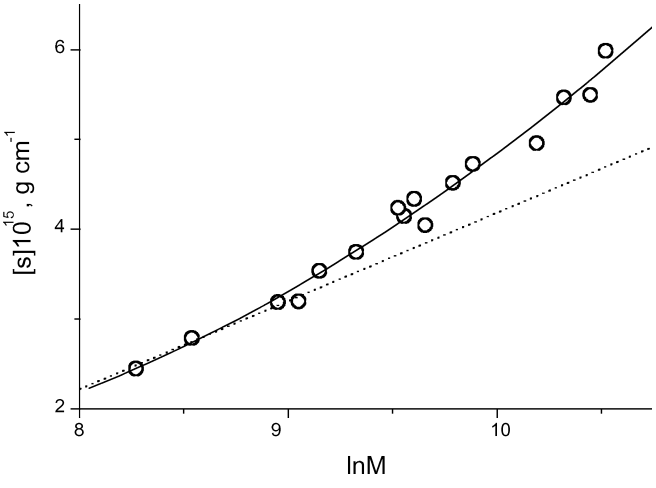

Fig. 11 Determination of M_L, the ratio of mass M to contour length L, and d, the hydrodynamic diameter, of heparin from the plot of $[s]$ vs. ln M. The intrinsic sedimentation coefficient $[s] \equiv s_0\eta 0/(\Delta\rho/\Delta c)$ and $M \equiv M_{SD}$ are obtained using analytical ultracentrifugation of heparin fractions. The linear extrapolation (*dotted line*) was made using the smallest fractions (V, 12, 13 and 14 of Table 1). The slope and intercept allows us to determine M_L and d, respectively, in the model of a weakly bending rod or a cylinder (see the text) usable in the theoretical limit of $L/A < 2.3$. This limit was determined using heparin fractions of larger size (see the text and Table 6)

Table 4 Comparison of M_L values of heparin chains obtained by different techniques

N	$(M_L \pm \Delta M_L)$ (g nm^{-1} mol^{-1})	Solvent	Techniques	Ref.
1	545	H_2O	Low-angle X-ray scattering	Stivala et al. (1968)
2	660	–	X-ray fibre diffraction	Atkins et al. (1974)
3	520 ± 40	H_2O	Low-angle X-ray scattering	Khorramian and Stivala (1986)
4	630 ± 20	H_2O	High-resolution NMR	Mulloy et al. (1993)
5	570 ± 50	0.2 M NaCl	Hydrodynamics	This work

Determination of the conformational parameters of heparin

Weakly bent rods as a model of heparin fractions of low molecular weight

At low molar mass, the dependency of $[s]$ versus $\ln M$ (Eq. 8, Fig. 11) was used to evaluate M_L and d. One obtains the estimates $M_L = 570 \pm 50$ g nm^{-1} mol^{-1}and $d = 0.9 \pm 0.15$ nm. The value of M_L is compared in Table 4 with those evaluated for heparin from other physical experiments (Stivala et al. 1968; Atkins et al. 1974; Khorramian and Stivala 1986; Mulloy et al. 1993). The difference between the M_L values of the table are more likely related to the experimental uncertainty of the various measurements than to the differences between the heparin samples. The M_L value from the present hydrodynamic method is very close to the mean value of 580 ± 50 g nm^{-1} mol^{-1}. From the mass per unit length, M_L, and the mean value of the disaccharide molecular weight obtained from the elementary analysis, $M_0 = 580$ g mol^{-1}, the length λ of the projection of the disaccharide in the main direction of the polymer chain may be calculated as $\lambda = M_0/M_L = 1.0$ nm. This value is very close to the value of 0.9 nm inferred from the three-dimensional NMR structure of a heparin fragment (Mulloy et al. 1993), as can be seen from Fig. 12.

Worm-like chain as a model of heparin macromolecules

The sets of hydrodynamic values, either $[s]$, $[\eta]$ or k_s, for the largest fractions ($L/A > 2.3$) plotted as a function of M (Eqs. 9, 10, 11) are used to obtain independent estimations of the Kuhn segment length$A$, characterizing the equilibrium chain rigidity, and the hydrodynamic diameter d. The models are that of a worm-like necklace or a worm-like cylinder. They do not consider the intramolecular volume interactions, which is justified in the limit $L/A < 50$ (Fujita 1988), and, in the present study, the values of L/A are always below 10, as can be inferred from Table 6. The determination of $d$requires the knowledge of the parameter $\phi(0)$, whose values are slightly different for the two considered models, i.e. worm-like necklace or worm-like cylinder. The estimations of the values of A and d obtained from the slopes and intercepts, respectively, of the plots of Fig. 13, using $P_0 = 5.11$ and $\Phi_0 = 2.87 \times 10^{23}$(Hearst and Stockmayer 1962; Yamakawa and Fujii 1974) are reported in Table 5. Using the sets of P_0 and Φ_0 values from Zimm (1980), Garcia de la Torre et al. (1984) or Oono and Kohmoto (1983) provides slightly reduced values for A from the experimental s_0 and M ($A = 8.7$ and 8.2 nm, respectively) and slightly larger values for A from the experimental $[\eta]$ and M ($A = 7.7$ and 8.0 nm, respectively). SAXS data allowed us to also obtain conformational parameters such as the cross-section diameter (from large-angle scattering; see the Results section) and the persistence length a ($a = A/2$). The evaluation of the persistence length was made from Fig. 14 by comparing theoretical curves of the radius of gyration as a function of the contour length (Eq. 15) with the experimental points. They are presented in Table 5 and compared with hydrodynamic results from the smallest and largest fractions.

Concerning the value of the Kuhn segment length A, the values of A obtained from translational and rotational frictions are in the same order of magnitude even if not identical, which is generally observed for linear polymers. They are close to the value obtained from SAXS. These A values reported in Table 5 are all obtained from the evolution of experimental structural characteristics (mentioned in the table) as a function of the molecular weights of heparin fractions. Our estimation of $A = 9 \pm 2$ nm is larger than that of 4.5 nm given using unfractionated heparin samples from SAXS but with a different procedure, by the determination of

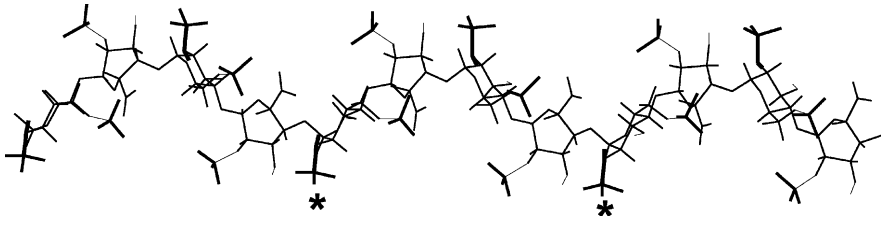

Fig. 12 High-resolution NMR structure of a heparin fragment of 12 saccharides. All chemical bonds are represented. This figure was drawn using the data of Mulloy et al. (1993) obtained from the Protein Data Bank. A distance of 1.75 nm between the two stars is measured, corresponding to 4 subsequent saccharides

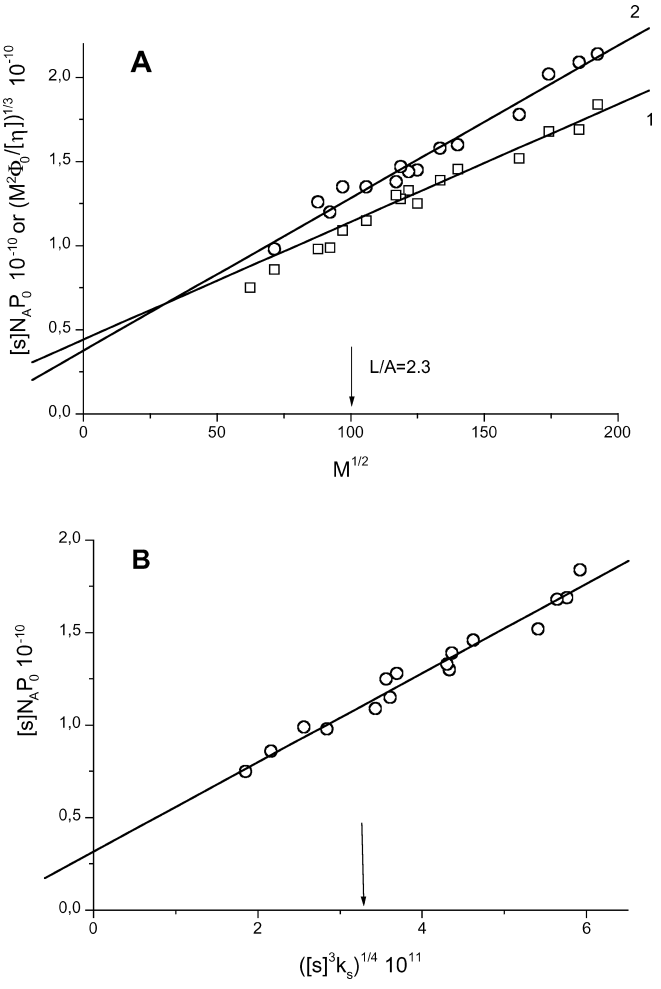

Fig. 13 Kuhn segment length A and hydrodynamic diameter d from hydrodynamic measurements on heparin fractions of different sizes. The dependencies of $[s]N_AP_0$(*squares*, *1*) and $(M^2\Phi_0/[\eta])^{1/3}$ (*circles*, *2*) on $M^{1/2}$ is shown in **A** and that of $[s]P_0N_A$on $[s]^{3/4}ks1^{/4}$ in **B**. The slope and the intercept of these curves may be used to evaluate A and d, respectively, in the framework of a worm-like necklace or a worm-like cylinder (see text). Their values are reported in Table 5. The data were obtained in 0.2 M NaCl at 20 °C

an inflection point on the $I(Q)Q^2$ scattering curve (Stivala et al. 1968; Khorramian and Stivala 1986). In view of our use of a set of fractions over a large range of molecular weights, which were well characterized with different experimental approaches, our estimation is likely to be more appropriate.

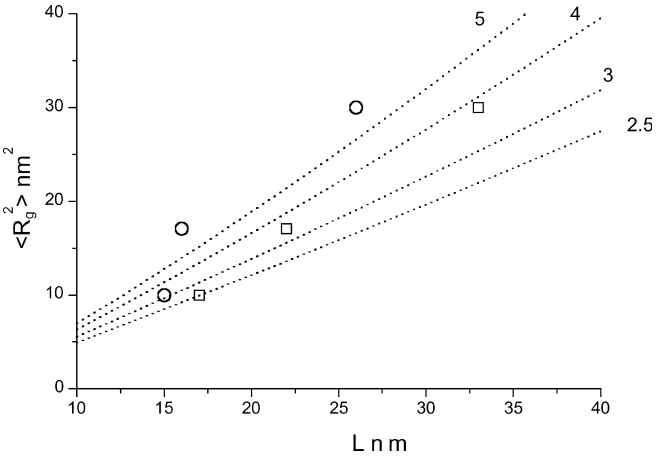

Fig. 14 Obtention of the persistence length of heparin from SAXS measurements. The evolution of the radius of gyration R_g from SAXS vs. the contour length L obtained by extrapolation of I_0 (*circles*) or $1/I_0$ (*squares*) for the fractions 4, 8 and 11 of heparin. *Dotted lines* are theoretical curves calculated according to Benoit and Doty (1953) for values of the persistence length of 5, 4, 3 and 2.5 nm

Concerning the transverse dimension, the hydrodynamic diameter obtained considering a worm-like cylinder model are slightly larger than that obtained with the worm-like necklace model, 0.9 nm and 0.7 nm, respectively. They have the same range of magnitude as the cross-section diameter obtained from SAXS (0.9 nm) and the maximum transversal dimensions (1 nm) in the three-dimensional NMR structure of a heparin fragment (Mulloy et al. 1993) (Fig. 11).

Conformations of the heparin fractions

For heparin considered as a homologous linear polymer we have determined the values for $M_L = 570$ g nm^{-1} mol^{-1}and $A = 12$, 7 or 9 nm from translational (D) or rotational ($[\eta]$) friction and SAXS data, and $d = 0.9$ nm. Heparin fractions can now be characterized as follows (Table 6): from M (Table 1) and M_L, the contour length $L = M/M_L$ is easily calculated. For each fraction, the contour length can be compared to the value of the Kuhn segment length. The number of Kuhn segments in the various heparin chains or relative contour length, $L/A = M/AM_L$, changes from 0.8 ± 0.2 for the fraction

Table 5 The Kuhn segment length$A$ and hydrodynamic diameter$d$ of heparin chains in 0.2 M NaCl

	$A \pm \Delta A$ (nm) Models of a worm-like necklace or a worm-like cylinder	$d \pm \Delta d$ (nm) Model of a worm-like cylinder	$d \pm \Delta d$ (nm) Model of a worm-like necklace
s_0, M ($L/A < 2.3$)	–	0.9 ± 0.15	–
s_0, M ($L/A > 2.3$)	12 ± 2	0.9 ± 0.15	0.7 ± 0.1
$[\eta]$, M ($L/A > 2.3$)	7 ± 0.7	0.7 ± 0.06	0.5 ± 0.04
s_0, k_s, β_s ($L/A > 2.3$)	9.5 ± 1.5	1.0 ± 0.2	0.7 ± 0.2
X-ray	9 ± 1	0.86 ± 0.02[a]	–

[a]This value corresponds to $2 < R_c^2 >^{1/2}$, with R_c the cross-section radius of gyration

Table 6 Mean conformation of the heparin fractions[a]

N	$M\times10^{-3}$ (g mol^{-1})	$N_{dissach}$ ($M_0=580$ g mol^{-1})	L (nm)	L/A ($A=9$ nm)	P ($d/A=0.08$)	$\Phi\times10^{-23}$ (mol) ($d/A=0.10$)	$<h^2>_{av}^{1/2}$ (nm)	$L/<h^2>_{av}^{1/2}$
1	37.0	64	66	7.3	3.83	1.29	25 ± 2	2.6
I_2	34.4	59	61.5	6.8	3.80	1.26	24.5 ± 2.5	2.5
2	30.3	52	54	6	3.74	1.21	22.5 ± 2.5	2.4
I	26.6	46	47.5	5.3	3.68	1.15	22 ± 2	2.2
4	19.6	34	35	3.9	3.54	1.03	18 ± 1	1.9
5	17.8	31	32	3.6	3.49	0.99	17.5 ± 1.5	1.8
II	15.6	27	28	3	3.43	0.94	17.5 ± 15	1.6
III	14.1	24	25	2.8	3.38	0.90	15.5 ± 1.5	1.6
8	13.7	24	24.5	2.7	3.7	0.89	15.5 ± 0.5	1.6
10	11.2	19	20	2.2	3.27	0.81	14 ± 1	1.4
11	9.4	16	17	1.9	3.19	0.75	12.5 ± 1.5	1.3
IV	8.5	15	15	1.7	3.14	0.72	12.5 ± 1.5	1.2
12	7.7	13	14	1.6	3.09	0.68	11.5 ± 1.5	1.2
13	5.1	9	9	1	2.93	0.55	(9 ± 1)	(1)
14	3.9	7	7	0.8	2.83	0.47	(9)	(1)

[a] $M_L=570$ g nm^{-1} mol^{-1}. M is the molecular weight, $N_{dissach}$ the number of disaccharides, L the contour length, A the Kuhn segment length, d the hydrodynamic diameter. $P=P(L/A,\ d/A)$ and $\Phi=\Phi(L/A,\ d/A)$ are tabulated hydrodynamic parameters (Yamakawa and Fujii 1974) for translational friction coefficient and intrinsic viscosity, respectively. They were used to determine end-to-end distances ($<h^2>^{1/2}$) indicated here as mean values (see text)

of the lowest molecular weight (fraction 14) to 7 ± 1.5 for the highest one (fraction 1).

This maximum value forL/A of 7 indicates a semi-rigid behaviour for the heparin molecules. Only the largest fractions ($M>30{,}000$ g mol^{-1}) may be considered as forming a penetrable coil. A real coil would correspond to L/A values above 15, a value that is not obtained even for the largest molecular weight fraction. The values of the scaling indices of heparin from hydrodynamic measurements in Table 3 are intermediate between those theoretically predicted considering excluded volume effects (non-draining coil) for the limiting cases of molecular flexibility and those predicted from the rod, while apparently closer to those of the coil than those of the rod (Fujita 1990). Rather than an appreciable flexibility, this may reflect the draining effects in heparin chains. From SAXS, $\delta=0.45$ values can be derived from the empirical power law$A_2\approx M^{-\delta}$ used for linear polymers. δ is in the range 0.2–0.3 for flexible polymers and increases to 0.5 for more rigid ones (Fujita 1990; Eskin 1986). This again supports our conclusion that heparin chains are semi-rigid macromolecules.

This range of relative contour lengths corresponds to large variations in the values of the hydrodynamic parameters P and Φ. The P and Φ values were obtained from the tables of Yamakawa and Fujii (1974), using $d/A=0.08$ and$d/A=0.10$ estimated from translational and rotational data, respectively, and the L/A values which characterize each fraction. They are reported in Table 6. They were used to determine the end-to-end distances $<h^2>^{1/2}$f and $<h^2>^{1/2}\eta$ according to Eqs. 2 and 1, respectively. The calculation of the end-to-end distances by these two ways leads to very similar estimations for all the fractions and the mean values are reported in Table 6. These mean values were used to calculate, for each fraction, the ratio between the contour length and the end-to-end distance, $L/<h^2>^{1/2}$. This allows an easy evaluation of the relative conformation of each fraction. A ratio of 1 corresponds to a rigid rod: it is obtained for the smallest fractions, which consist of less than 10 disaccharides. The ratio increases with the size of the polymer, reaching values above 2 for more than 50 disaccharides.

Interestingly, it can be calculated for heparin in our solvent conditions (0.2 M NaCl, $\lambda_B=0.7$ nm^{-1}, $\kappa^{-1}=0.7$ nm^{-1}, $L/Z=0.47$ nm, $Q_{el}=1.5$) that the electrostatic contribution, A_{el}, to the Kuhn segment length of heparin is only 0.35 nm. This is clearly 1–2 orders of magnitude smaller than the experimental estimation of A. It means that the total chain rigidity of heparin, unless at very low solvent salt concentration (below 0.01 M, where $A_{el}\approx7$ nm), is determined by a structural rigidity contribution. This is in agreement with the fact that the concentration dependency of the viscosity of heparin does not vary significantly for solvents containing NaCl above 0.05 M (to be published elsewhere). From this analysis, the rigidity of heparan sulfate and heparin molecules, which differ essentially in their charge densities, is expected to be virtually the same, even if local interactions of course can determine a specific folding of the polysaccharide. The conformational lability of iduronic acid was claimed to explain the specific interaction capabilities of glycosaminoglycans (Rees et al. 1985; Casu et al. 1988).

Conclusion

Heparin fractions in the range 4000–37,000 g mol^{-1} that were obtained from column gel permeation chromatography presented the behaviour of an homologous series of linear macromolecules. Within these fractions,

those of small relative contour lengths were characterized using the theory of a weakly bending rod in order to estimate the mass per length unit. It has to be noted that this structural characteristic, M_L, can only exceptionally be obtained from hydrodynamic data, because it requires small macromolecules of different lengths. The knowledge of M_L allows us to obtain further quantitative estimations of conformational parameters of the polysaccharide using the fractions with the largest range of molecular weights. The hydrodynamic behaviour of heparin in 0.2 M NaCl is described adequately by the worm-like chain model with a Kuhn segment length of $A = 9 \pm 2$ nm and a hydrodynamic diameter of $d = 0.9 \pm 0.1$ nm. SAXS confirmed these dimensions. Considering all known polymers, A values are found in the range 1–200 nm (Pavlov et al. 1999). Linear macromolecules are rigid for large values of A (> 10 nm) and flexible for small values (1–3 nm). The 7–12 nm value found for heparin corresponds to a semi-rigid macromolecule.

Acknowledgements G.P. and E.K. are indebted and grateful to the CEA (Grenoble, France) for the opportunity to work in the Institute of Structural Biology. Thanks are due to Hugues Lortat-Jacob (IBS) for stimulating discussions and advice; to Barbara Mulloy (NIBSC, UK) for analytical gel permeation chromatography experiments and discussions of the results; and to Céline Pellissier for technical assistance.

References

Atkins EDT, Isaac DH, Nieduszynski IA, Phelps CF, Sheehan JK (1974) The polyuronides: their molecular architecture. Polymer 15:263–271

Barlow GH, Sanderson ND, McNeill PD (1961) Macromolecular properties and biological activity of heparin. Arch Biochem Biophys 84:518–525

Barrat JL, Jonny JF (1996) Theory of polyelectrolyte solutions. Adv Chem Phys 94:1–43

Benoit H, Doty PM (1953) Light scattering from non-Gaussian chains. J Phys Chem 57:958–963

Broersma S (1969) Translational diffusion constant of a random coil. J Chem Phys 51:233–238

Bushin SV, Tsvetkov VN, Lysenko EB, Emeliyanov VN (1981) Conformation properties and rigidity of molecules of ladder polyphenylsiloxane in solutions according the data of sedimentation-diffusion analysis and viscometry. Vysokomol Soedin Ser A 23:2494–2503

Cantor CR, Schimmel PR (1980) Biophysical chemistry. Freeman, San Francisco

Casu B (1985) Structure and biological activity of heparin. Adv Carbohydr Chem Biochem 43:51–134

Casu B, Lindahl U (2001) Structure and biological interactions of heparin and heparan sulfate. Adv Carbohydr Chem Biochem 57:159–206

Casu B, Petitou M, Provasoli M, Sinay P (1988) Conformational flexibility: a new concept for explaining binding and biological properties of iduronic acid-containing glycosaminoglycans. Trends Biochem Sci 13:221–225

Costenaro L, Zaccai G, Ebel C (2001) Understanding the crystallisation of an acidic protein by dilution in the ternary NaCl–2-methyl-2,4-pentanediol–H_2O system. J Cryst Growth 232:102–113

Eskin V (1986) Light scattering by polymer solutions and macromolecular properties. Science, Leningrad

Fujita H (1988) Some unsolved problems of dilute polymer solutions. Macromolecules 21:179–185

Fujita H (1990) Polymer solutions. Elsevier, Amsterdam

Garcia de la Torre J, Martinez MCL, Tirado MM, Freire JJ (1984) Monte Carlo study of hydrodynamic properties of flexible linear chains: analysis of several approximate methods. Macromolecules 17:2715–2722

Glatter O, Kratky O (eds) (1982) Small angle X-ray scattering. Academic Press, London

Gotlib Yu, Darinskiy A, Svetlov Yu (1986) Physical kinetics of macromolecules. Chemistry Press, Leningrad

Guinier A, Fournet G (1955) Small-angle scattering of X-rays. Wiley, New York

Hearst JE, Stockmayer WH (1962) Sedimentation constants of broken chains and wormlike coils. J Chem Phys 37:1425–1432

Hileman RE, Fromm JR, Weiler JM, Linhardt RJ (1998) Glycosaminoglycan–protein interactions: definition of consensus sites in glycosaminoglycan binding proteins. BioEssays 20:156–167

Khorramian BA, Stivala SS (1986) Small-angle X-ray scattering of high- and low-affinity heparin. Arch Biochem Biophys 247:384–392

Knobloch JE, Shaklee PN (1997) Absolute molecular weight distribution of low-molecular-weight heparins by size-exclusion chromatography with multiangle laser light scattering detection. Anal Biochem 245:231–241

Kratky O, Leopold H, Stabinger H (1973) The determination of the partial specific volume of proteins by the mechanical oscillator technique. Methods Enzymol 27:98–110

Landau LD, Lifschitz EM (1963) Statistical physics, 3rd edn. Pergamon Press, Oxford

Lane DA, Lindahl U (eds) (1989) Heparin. Chemical and biological properties, clinical applications. CRC Press, Boca Raton, Florida

Lane DA, Bjork I, Lindahl U (eds) (1992) Heparin and related polysaccharides. (Advances in experimental medicine and biology) Plenum Press, New York

Lasker SE, Stivala SS (1966) Physico-chemical studies of fractionated bovine heparin. Some dilute solution properties. Arch Biochem Biophys 115:360–372

Laurent TC (1961) Studies on fractionated heparin. Arch Biochem Biophys 92:224–231

Liberti PA, Stivala SS (1967) Physico-chemical studies of fractionated bovine heparin. Viscosity as a function of ionic strength. Arch Biochem Biophys 119:510–518

Lindahl U (2000) Heparin from anticoagulant drug into the new biology. Glycoconjug J 17:597–605

Lindner P, Zemb T (eds) (1991) Neutron, X-ray and light scattering: introduction to an investigative tool for colloidal and polymeric systems. North-Holland, Amsterdam

Liu J, Thorp SC (2002). Cell surface heparan sulfate and its roles in assisting viral infections. Med Res Rev 22:1–25

Liu D, Shriver Z, Venkataraman G, El Shabrawi Y, Sasisekharan R (2002) Tumor cell surface heparan sulfate as cryptic promoters or inhibitors of tumor growth and metastasis. Proc Natl Acad Sci USA 99:568–573

Lortat-Jacob H, Balzer F, Grimaud JA (1996) Heparin decreases the blood clearance of interferon-gamma and increases its activity by limiting the processing of its C-terminal sequence. J Biol Chem 271:16139–16143

Lortat-Jacob H, Grosdidier A, Imberty A (2002) Structural diversity of heparan sulfate binding domains in chemokines. Proc Natl Acad Sci USA 99:1229–1234

Loucas SP, Yeh KC, Haddad HM (1971) Effect of calcium ions on the scattering of light by heparin. J Pharm Sci 60:1109–1111

Mandel M (1993) Some properties of polyelectrolyte solutions and the scaling approach. In: Hara M (ed) Polyelectrolytes: science and technology. Dekker, New York, pp 1–75

Mandelkern L, Flory PJ (1952) The frictional coefficient for flexible chain molecules in dilute solution. J Chem Phys 20:212–214

Miklautz H, Riemann J, Vidic HJ (1986) The molecular weight distribution of heparin determined with a HPLC-LALLS coupling technique. J Liq Chromatogr 9:2073–2093

Mulloy B, Forster MJ (2000) Conformation and dynamics of heparin and heparan sulfate. Glycobiology 10:1147–1156
Mulloy B, Forster MJ, Jones C, Davies DB (1993) N.m.r. and molecular-modeling studies of the solution conformation of heparin. Biochem J 293:849–858
Mulloy B, Gee C, Wheeler SF, Wait R, Gray E, Barrowcliffe TW (1997) Molecular weight measurements of low molecular weight heparins by gel permeation chromatography. Thrombosis Haemostasis 77:668–674
Narayanan T, Diat O, Bösecke P (2001) SAXS and USAXS on the high brilliance beamline at the ESRF. Nucl Instrum Methods A 467–468:1005–1009
Nieduszynski I (1989) General physical properties of heparin. In: Lane DA, Lindahl U (eds) Heparin. Chemical and biological properties, clinical applications. CRC Press, Boca Raton, Florida, pp 51–63
Odijk T (1977) Polyelectrolytes near the rod limit, J Polym Sci Polym Phys Ed 15:477–485
Oono Y, Kohmoto M (1983) Renormalization group theory of transport properties of polymer solutions. I. Dilute solutions. J Chem Phys 78:520–528
Pavlov GM (1997) The concentration dependence of sedimentation for polysaccharides. Eur Biophys J 25:385–397
Pavlov GM, Frenkel SYa (1995) Sedimentation parameter of linear polymers. Prog Colloid Polym Sci 99:101–108
Pavlov GM, Harding SE, Rowe AJ (1999) Normalized scaling relations as a natural classification of linear macromolecules according to size. Prog Colloid Polym Sci 113:76–80
Rees DA, Morris ER, Stoddart JF, Stevens ES (1985) Controversial glycosaminoglycan conformations. Nature 317:480
Solovyova A, Schuck P, Costenaro L, Ebel C (2001) Non-ideality by sedimentation velocity of halophilic malate dehydrogenase in complex solvents. Biophys J 81:1868–1880
Spillmann D (2001) Heparan sulfate: anchor for viral intruders? Biochimie 83:811–817
Stivala SS, Herbst M, Kratky O, Pilz I (1968) Physico-chemical studies of fractionated bovine heparin V. Some low-angle X-ray scattering data. Arch Biochem Biophys 127:795–802
Sugahara K, Kitagava H (2000) Recent advances in the study of the biosynthesis and functions of sulfated glycosaminoglycans. Curr Opin Struct Biol 10:518–527
Svedberg T, Pedersen KO (1940) The ultracentrifuge. Oxford University Press, Oxford
Tanford C (1961) Physical chemistry of macromolecules. Wiley, New York
Theisen A, Johann C, Deacon MP, Harding SE (2000) Refractive increment data-book. Nottingham University Press, Nottingham
Tsvetkov VN (1989) Rigid-chain polymers. Consultants Bureau, New York
Tsvetkov VN, Klenin SI (1953) Diffusion of polystyrene fractions in dichlorethane. Dokl Akad Nauk SSSR 88:49–51
Tsvetkov VN, Eskin VE, Frenkel SYa (1970) Structure of macromolecules in solutions. Butterworths, London
Tsvetkov VN, Lavrenko PN, Bushin SV (1984) Hydrodynamic invariant of polymer molecules. J Polym Sci Polym Chem Ed 22:3447–3460
Weast RC (ed) (1975) Handbook of chemistry and physics, 56th edn. CRC Press, Cleveland
Yamakawa H (1971) Modern theory of polymer solutions. Harper and Row, New York
Yamakawa H, Fujii M (1973) Translational friction coefficient of wormlike chains. Macromolecules 6:407–415
Yamakawa H, Fujii M (1974) Intrinsic viscosity of wormlike chains. Determination of the shift factor. Macromolecules 7:128–135
Zimm B (1980) Chain molecule hydrodynamics by the Monte-Carlo and the validity of the Kirkwood-Riseman approximation. Macromolecules 13:592–602